PART THREE

Design Strategy and Methodology

7 Detailed rudder design

7.1 Background and philosophy of design approach

The forces developed by a rudder or control surface depend fundamentally on its area, profile shape and aspect ratio (ratio of span to chord), section shape, the square of the inflow velocity, the density and viscosity of water and the rudder angle of attack or incidence α. These parameters are described in Section 3.4.2 and, for a precise estimate of the rudder forces all of the parameters have to be taken into account.

Classical approaches to rudder design have tended to concentrate mainly on the derivation of rudder torque and a suitable stock diameter. Rudder force and its centre of pressure were derived using empirical equations that were based on relatively limited model- and full-scale data. Derived equations are of the form:

$$\text{Force } N = kf_1(\alpha)AV^2$$

$$CPc = f_2(\alpha)AV^2$$

$$\text{Torque } Q_R = N \times \text{lever of stock position to } CPc$$

In early formulae, $f_1(\alpha)$ is a function of the rudder angle only and does not take account of aspect ratio, although later formulae would allow for this in the constant k. Many alternatives for $f_1(\alpha)$ are listed by Kinoshita [7.1], and a popular choice was $\sin\alpha$. Another assumption was to take $CPc = 0.375\bar{c}$ at 35° rudder angle.

Jöessel [7.2] carried out tests on plate rudders in 1873 in the Loire river and derived empirical formulae for rudder torque and centre of pressure as follows:

$$\text{Torque } Q_R = 405.8\,AV^2 \sin\alpha\,\bar{c}$$

$$CPc = (0.195 + 0.305\sin\alpha)\bar{c}$$

and

$$\text{Force } N = 405.8\,AV^2\left[\frac{\sin\alpha}{0.195 + 0.305\sin\alpha}\right]$$

These formulae were used extensively for many years, with different values of the coefficient developed for various ship and rudder types. Mention should also be made of the extensive early experimental work carried out on rudders by Denny [7.3], Baker and Bottomley [7.4–7.9], Abell [7.10] and Gawn [7.11] and their

proposals for empirical equations for force and centre of pressure. Many of the results of Baker, Bottomley, Abell and Denny are summarised and discussed by van Lammeren *et al.* [7.12], together with the results of several rudder tests carried out in the Wagengingen test tank. Equations due to Baker, Bottomley and Gawn include:

For twin screw-twin rudders, Gawn [7.11]:

$$\text{Force } N = 21.1\ AV^2\alpha$$

For single screw-single rudder, Baker and Bottomley [7.4]:

$$\text{Force } N = 18.0\ AV^2\alpha$$

Attwood and Pengelly [7.13] give a good description of the application of such empirical formulae for forces and centre of pressure. For nonrectangular rudders, such as Figure 7.1(a), the forces on each rectangle can be calculated as though they acted independently and the forces then combined to give the total force. For the centre of pressure of nonrectangular rudders such as Figure 7.1(b), the recommended method is to divide the rudder into a number of horizontal strips, each considered as a rectangle with its own *CPc*. Using quadrature across the span, the moments of area of each strip are summed to give the total moment; this is divided by the total area to give the centre of pressure. Applying the total force from a formula (such as above), multiplied by the appropriate lever from the centre of pressure to the position of the stock, provides the total torque. Attwood and Pengelly emphasise the need to include frictional losses in the rudder bearings and to check the astern torque.

A practical approach using such data and methods is described by Lamb and Cook [7.14].

A thorough review of the hydrodynamic aspects of appendage design is presented by Mandel [7.15] including, in particular, the important aspects concerned with the design of rudders.

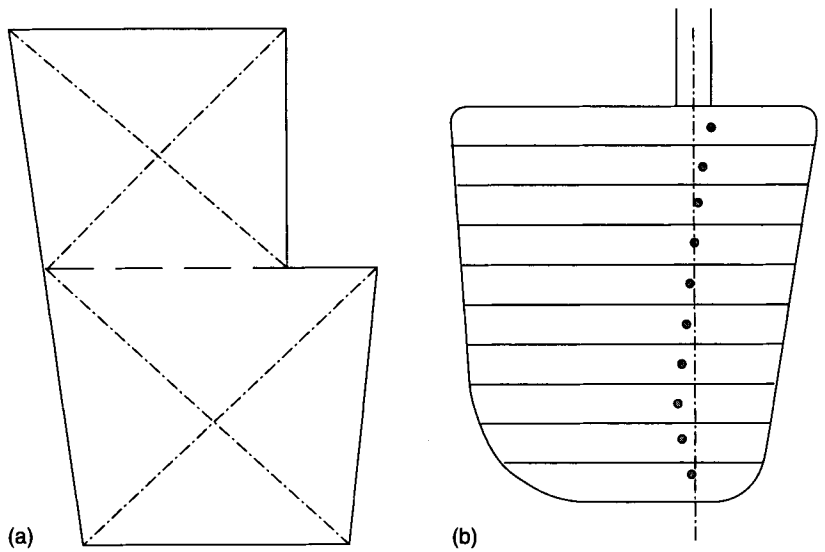

Figure 7.1 Nonrectangular rudders [7.13]

Jaeger [7.16] presents methods and calculations for rudder torque prediction that include the use of wind tunnel data and the incorporation of the influence of aspect ratio. Estimates of propeller-induced velocities are included based on propeller apparent slip values.

Gover and Olsen [7.17] present a method for predicting the torque of semi-balanced centreline rudders on multiple screw ships, that is with the rudder not in a propeller slipstream. The rudder is broken down into two parts A_1 and A_2, Figure 7.2, each with *CPc* distance x_1 and x_2 from the leading edge. Curves are provided for normal force coefficient C_N and centre of pressure *CPc* based on the aspect ratio of each portion. The method shows reasonable agreement with the experimental results of Hagen [7.18].

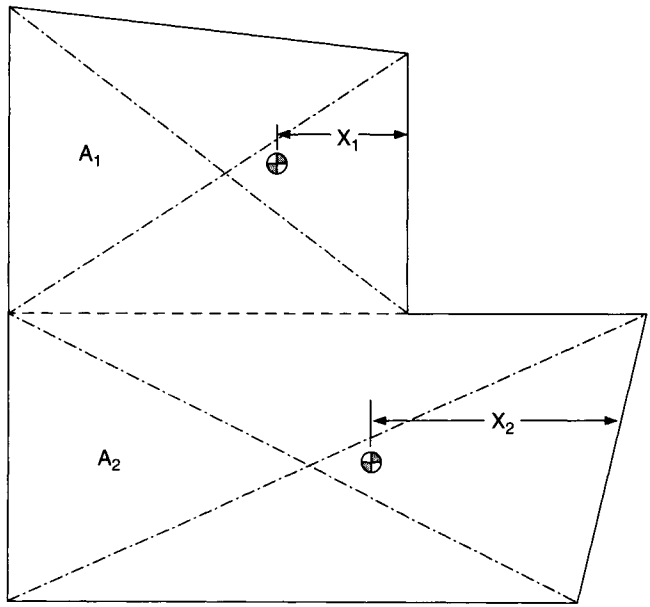

Figure 7.2 Semi-balanced centreline rudder [7.17]

A significant change in the level of understanding of the behaviour of control surfaces, with relatively low aspect ratio suitable for marine applications, occurred with the publication of the extensive free-stream tests of Whicker and Fehlner [7.19]. An early publication using the results of Whicker and Fehlner, and a more rigorous approach to rudder forces, torques and moments, was that of Taplin [7.20]. He includes example calculations to illustrate the methodology. Other publications of note through that period include those of Romahn and Thieme [7.21], Thieme [7.22] and Okada [7.23].

Harrington [7.24] presents an extensive review of rudder torque prediction. He makes use of the Whicker and Fehlner data, also comparing the results with the Jöessel method. He includes estimates of the frictional losses in the rudder bearings and compares his results with full-scale measurements.

In the field of yachts and small powercraft, relevant publications on rudder design include those of Millward [7.25] and Molland [7.26].

The manual of Brix [7.27] presents a wide range of detailed information concerning the design of rudders of many types. It also includes a thorough review of other manoeuvring devices.

Son *et al.* [7.28] and Kresic [7.29] present methods for estimating the torque of semi-balanced skeg, or horn, rudders. Son *et al.* use the modified lifting line analysis of Molland [7.30] for the prediction of forces and *CPc* and carried out a regression analysis of the results. Satisfactory agreement with full-scale data was obtained. Kresic developed a program for detailed estimates of torque for skeg rudders. He compared his results with model data, including the free-stream work of Goodrich and Molland [7.31].

It can be seen that the publication of the free-stream characteristics of various rudder series, including all-movable, flapped and semi-balanced skeg rudders, has enabled a more rigorous analysis and physically correct approach to be used for the design of marine rudders and control surfaces. Consequently, the most common rudder design and performance prediction method currently employed entails the use of free-stream or open-water characteristics for a particular rudder or control surface. The free-stream characteristics of the rudder represent its performance in the absence of the hull, propeller, or appendages. In order to take account of the presence of the hull and/or propeller, corrections are applied to the rudder aspect ratio, the inflow velocity to the rudder and to the rudder angle of attack to yield their effective values. These effective values are then used to enter the appropriate free-stream characteristic curves, and hence to compute the rudder forces and moments. The rudder in the free-stream condition and the modifying effects on the free stream of the hull and propeller are, therefore, treated as individual components of the complete system. This approach is discussed further in Section 7.2.

A number of mathematical models of rudder–propeller interaction using the individual component approach have been developed over the years, generally using actuator disc theory (Section 3.6), to model the rudder axial inflow velocity. This approach, together with a relatively large number of empirical modifications, can achieve reasonable predictions in simulations. The method of using free-stream characteristics with correction factors is, however, deficient in that it does not correctly account for the actual physical interaction between the various components including, for example, the asymmetric performance of a rudder downstream of a propeller, the spill over effects when the propeller slipstream is not completely covering the rudder span, or the significant increase in stall angle when the rudder is downstream of a propeller. Consequently, test data have been derived in various investigations for the rudder–propeller combination working as a unit. In this case, the rudder plus propeller is modelled as a combination in isolation, taking account of the governing parameters described in Section 3.5.2. The influences of an upstream hull and drift angle β are then applied in the form of velocity and flow straightening inputs to the basic isolated model of the rudder–propeller combination. The feasibility of this approach has been demonstrated through experimental work, Molland and Turnock [7.32], which has indicated, for example, that a systematic change in drift angle applied to the rudder–propeller combination leads to an effective shift in the sideforce characteristics of the combination by an angular offset, Figure 5.93, Section 5.4.2.7. Thus if these stages in the procedure are modelled in the manner described, with sufficient detail and adequate accuracy,

then a versatile and more physically correct model of rudder action in the presence of a propeller can be established. Example applications using this approach are included in Chapter 11. A design methodology using the rudder–propeller interaction data of Molland and Turnock is presented by Smithwick [7.33] and Molland *et al.* [7.34].

7.2 Rudder design process

In the process of designing a rudder it is necessary to identify the performance and design requirements, choose and apply a rudder with appropriate geometric parameters and estimate its performance characteristics for the given flow conditions. The overall rudder design process may then be summarised as follows:

Input rudder parameters

(i) Number of rudders
(ii) Rudder type
(iii) Area
(iv) Aspect ratio
(v) Profile shape: taper ratio and sweep
(vi) Chordwise section shape and thickness
(vii) Position of stock, balance
(viii) Rudder location relative to hull
(ix) Rudder location relative to propeller

Input flow conditions

(i) Effective inflow velocity
(ii) Effective rudder incidence

Output data

(i) C_L over range of incidence
(ii) C_D over range of incidence
(iii) C_{Lmax}
(iv) α_{stall}
(v) Centre of pressure
(vi) Pressure (load) distribution

Outcomes

The output data are used to derive rudder torque and bending moments to size the rudder stock diameter, size the steering gear, estimate rudder scantlings from the load distributions and provide lift and drag data for coursekeeping and manoeuvring simulations. An outline of the overall rudder design flow path is shown in Figure 7.3.

The following section discusses the topics within the design process:

7.2.1 Rudder parameters

Number. The number of rudders will depend on the ship type and service, or yacht or boat size and purpose. In motor-propelled vessels, the number of rudders

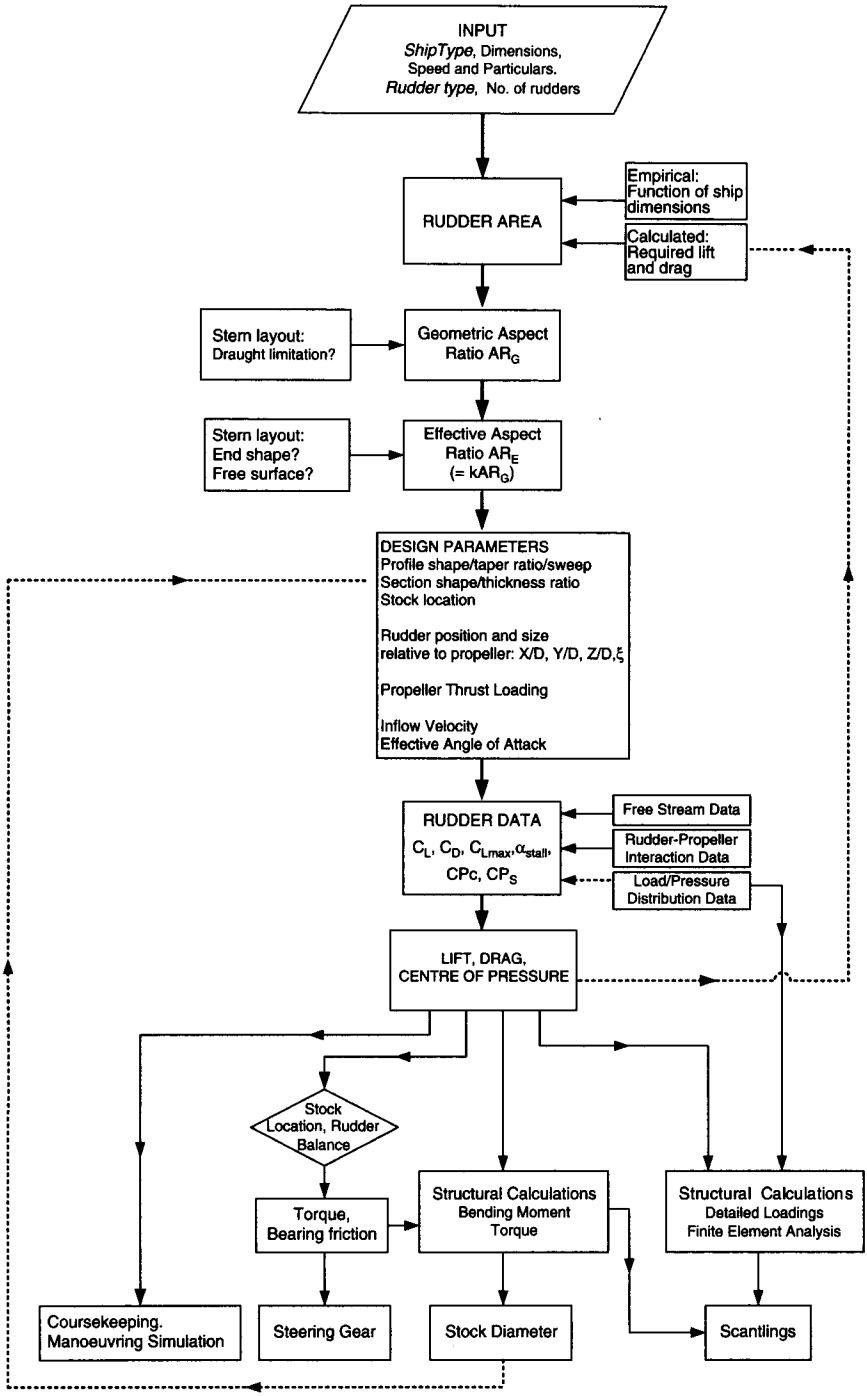

Figure 7.3 Rudder design flow path

will generally follow the number of propellers. In sailing yachts, the number will depend on the required total rudder area and performance requirements.

Type. Typical rudder types are shown in Figure 2.2, Section 2.2. The rudder type chosen will often be related to the ship type and stern arrangement. There are, however, circumstances where alternatives may be available, such as the choice between an all movable spade-type rudder, a full-skeg rudder, or a semi-balanced skeg rudder. Typical reasons for choosing the alternatives include hydrodynamic performance, structural design, layout and maintenance.

Area. Rudder area would ideally be estimated using a coursekeeping and manoeuvring simulation that would indicate the size of the rudder necessary to provide a certain level of steering performance. In practice, this is generally not possible at the preliminary design stage when the stern arrangement, propeller and rudder layouts are being decided. An alternative, and often used procedure, is to estimate the area, generally based on a proportion of the immersed lateral area, from the area used for similar ships with satisfactory steering properties (see Section 5.6). This has been found to be a satisfactory procedure for existing ship types and aft end layouts. Care must however be exercised if radical changes to the aft end layout are applied, when more fundamental investigations may be necessary including model tests and simulations.

Aspect ratio. Aspect ratio may be deemed the most important parameter as far as hydrodynamic performance is concerned, with increase in aspect ratio leading to an increase in overall hydrodynamic efficiency of the control surface. In merchant ships, aspect ratio tends to evolve as a result of the rudder–propeller layout. For example, if there are any draught limitations, then maintaining a required rudder area will lead to an increase in rudder chord length and decrease in aspect ratio. Such low aspect ratios can be seen on shallow draught inland waterway vessels. The shape of the hull above the rudder is important in that it affects the aspect ratio used for the performance predictions. It should be noted that an increase in aspect ratio for a spade rudder can lead to conflicting outcomes since it will lead to an increase in rudder root bending moment, increase in root thickness for structural reasons and a consequent decrease in hydrodynamic performance. Such a scenario in the case of a sailing yacht is addressed in example application 13 in Chapter 11.

Profile shape. Profile shape tends not to have a significant influence on hydrodynamic performance (see Section 5.3.2). Small amounts of taper and sweep tend to be the norm. Further adjustments to shape may occur to suit particular stern arrangements.

Section shape. The choice of chordwise section shape will follow design requirements for hydrodynamic performance. Standard aerofoil type sections are used in most cases, but specialised sections may be employed where increased lift curve slope, delayed stall, low drag or the avoidance of cavitation is sought (see Sections 5.3.2 and 5.8.4). Numerical methods can be usefully employed in the design of section shapes (Chapter 6). Section thickness generally results from structural requirements.

Balance. Balance can be fundamental to the rudder design since it influences tiller forces and steering gear size. However, as the centre of action of the forces (centre of pressure) moves aft with increase in incidence, it is generally not possible to

fully balance a rudder or control surface over a range of incidence. The location of the stock will depend on whether the centre of pressure should always be aft of the stock, which would lead to a trailing rudder in the event of a tiller or a steering gear malfunction, but with relatively high torques at large incidence, or a compromise where some negative torque is accepted at small angles in order to lower peak torques at large angles. In this case, the rudder will flop over and increase in angle of attack in the event of a tiller or steering gear malfunction. In order to limit an excessive size of steering gear, this tends to be the practice for large merchant ships. In the case where astern operation is important, such as for some ferries and warships, a compromise stock position may have to be adopted to achieve peak ahead and astern torques at broadly the same level. Example applications in Chapter 11 illustrate the effects of change in the position of the stock on torque.

Rudder-hull. The rudder location relative to the hull can be important as it may influence the end effect between the rudder and the hull, the effective aspect ratio and, consequently, hydrodynamic performance (see Section 5.5).

Rudder-propeller. The rudder location relative to the propeller influences the performance of the rudder depending on the relative longitudinal locations, the amount of asymmetry in the propeller race and the proportion of the rudder within the propeller race, as described in Sections 5.4 and 5.9. The whole propeller diameter will, where possible, be within the rudder span to utilise fully the accelerated flow from the propeller. In practice, this may not always be achievable, such as the case of some small twin-screw ships, Figure 4.8. A discussion of the influences of the relative positions of the rudder and propeller on performance is included as example application 9 in Chapter 11.

7.2.2 Flow conditions

Velocity. In the case of a sailing craft, or a twin-screw motor ship with a rudder not in way of the propellers, the effective inflow velocity will be estimated by taking into account the slowing down effect of the hull (Section 3.7). In the case where the rudder is operating downstream of a propeller, this will amount to estimating the slowing down effect of the hull on the propeller, together with the accelerating effect of the propeller on the flow into the rudder, Sections 3.5 and 3.6. Where performance data are available for the rudder operating downstream of a propeller, such as the experimental data presented in Section 5.4, the data are entered at the appropriate propeller thrust loading, K_T/J^2. Alternatively, the propeller induced velocity, Sections 3.5, 3.6, is applied directly to the free-stream rudder data, Section 5.3.

Incidence. The effective inflow incidence on a control surface is likely to be different from the set incidence. For a sailing craft, the rudder can often be operating in the downwash of the keel. For a ship or a boat just entering a turn, the hull develops a drift or leeway angle which decreases the effective rudder angle, whilst the hull and the propeller have flow straightening effects, which increase the effective angle (see Section 5.4.2.7). These factors will be taken into account in manoeuvring simulations and may be considered in the preliminary rudder design process.

7.2.3 Output data

For given effective inflow velocity and incidence, performance data will be obtained and applied for the control surface type and size under consideration. The sources of an extensive range of such performance data are described in Chapters 5 and 6.

7.2.4 Outcomes

The output data can be used in a systematic way to estimate the forces acting on the rudder, to estimate the diameter of the rudder stock and to size the steering gear. The data will broadly be applied in the following manner:

(A) *Forces, torques, moments*: Levers of centres of centre of pressure, Figure 5.1:

$$\bar{x} = \left[\frac{CPc}{100} \times \bar{c}\right] - x_1$$

$$= \left[\frac{CPc}{100} - \frac{x_1}{100}\right] \times \bar{c} \tag{7.1}$$

$$\bar{y} = \frac{CPs}{100} \times S \tag{7.2}$$

Force data:

$$C_N = C_L \cos\alpha + C_D \sin\alpha \tag{7.3}$$

where α is the effective rudder incidence

Normal force $$N = C_N \times 0.5\,\rho A V^2 \tag{7.4}$$

Rudder torque $$Q_R = N \times \bar{x} \tag{7.5}$$

Typical curves of CPc, C_N and Q_R are shown in Figure 7.4. In the example shown, the rudder has some balance and the stock axis has been chosen whereby there is some negative torque at low angles of attack, leading to a lower maximum (positive or negative) torque.

Resultant force coefficient: $$C_R = \sqrt{C_L^2 + C_D^2} \tag{7.6}$$

and resultant force $$R = C_R \times 0.5\,\rho A V^2 \tag{7.7}$$

Root bending moment (spade rudder case)

$$M = R \times \bar{y} \tag{7.8}$$

Equivalent bending moment

$$BM_E = \frac{M}{2} + 0.5\sqrt{M^2 + Q_R^2} \tag{7.9}$$

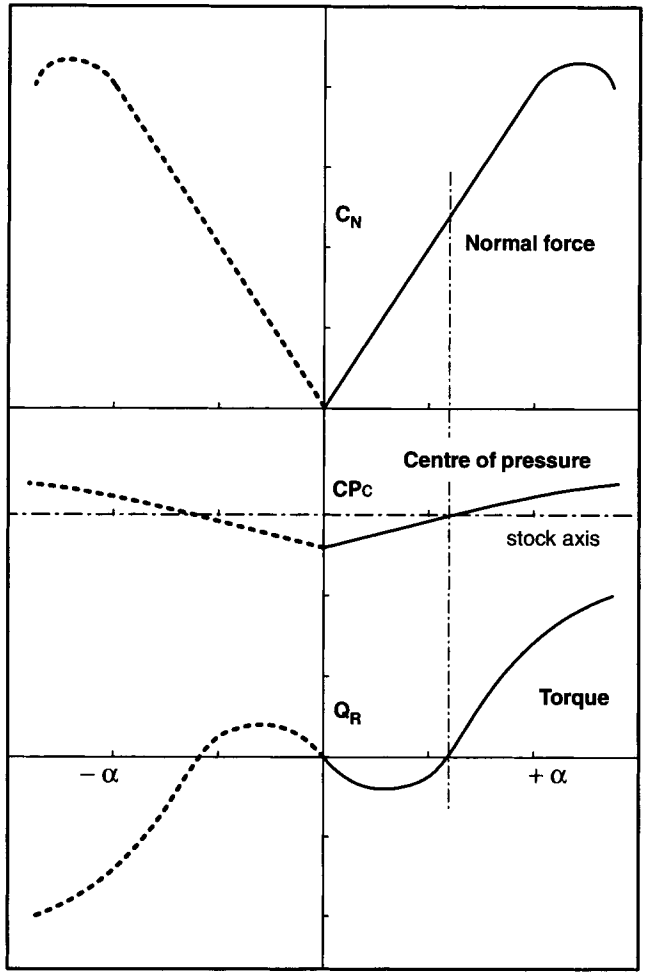

Figure 7.4 Typical curves of rudder normal force C_N, centre of pressure *CPc* and torque Q_R

Equivalent torque

$$Q_{RE} = M + \sqrt{M^2 + Q_R^2} \tag{7.10}$$

Diameter of rudder stock

$$D = \sqrt[3]{(BM_E \times 32)/\pi \times \sigma} \quad \text{or} \quad = \sqrt[3]{(Q_{RE} \times 16)/\pi \times \sigma} \tag{7.11}$$

where σ is the allowable stress in the stock material.

For an equivalent tubular rudder stock, the outside and inside diameters d_1 and d_2 have to satisfy the equation:

$$D = \sqrt[3]{(d_1^4 - d_2^4) / d_1} \tag{7.12}$$

Use of these formulae is illustrated in the example applications in Chapter 11.

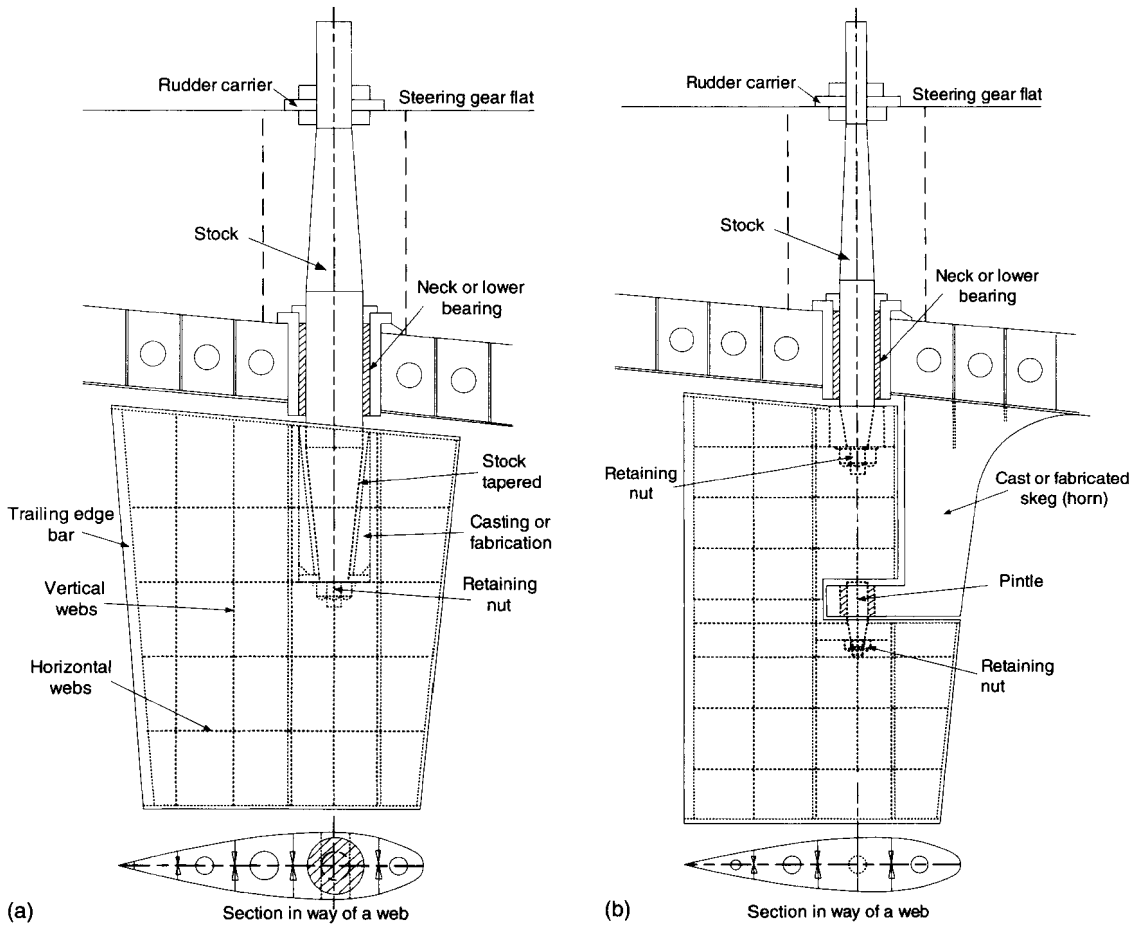

Figure 7.5 (a) Structural layout: spade rudder; (b) Structural layout: skeg rudder

(B) *Load distributions and scantlings*: Examples of outline structural layouts for a spade rudder and a semi-balanced skeg rudder are shown in Figure 7.5.

The scantlings for the rudder webs and plating will normally be obtained or checked using the rules of classification societies and standards such as references [7.35–7.40]. Direct calculations may also be carried out. In this case, the load distributions can be established from available experimental pressure distributions such as those described in Section 5.4.2.3, or one of the numerical methods described in Chapter 6. These load distributions may then be linked to a finite element analysis, FEA, which will determine the structural response of the rudder to the prescribed load distribution. This will allow appropriate structural scantlings for the rudder to be determined. Derived rudder scantlings, together with the derived stock diameter, will then normally be compared with the requirements of the various classification societies and standards. The application of an FEA package to a prescribed distribution of rudder loading is illustrated in example application 8 in Chapter 11.

(C) *Steering gear*: The rudder characteristics determine the hydrodynamic torque, Q_H, which is effectively Q_R in Equation (7.5) and Figure 7.4. The frictional torque Q_F due to friction in the rudder bearings also has to be overcome. The total torque Q_T to be provided by the steering gear is

$$Q_T = Q_F \pm Q_H \tag{7.13}$$

The sign in equation (7.13) depends on whether the rudder angle is being displaced or restored. The effect of friction and whether the rudder angle is being displaced or restored is shown schematically in Figure 7.6. This shows the basic hydrodynamic torque Q_H, say Q_R from Figure 7.4, together with Q_F to give the total torque Q_T. As the rudder is displaced, with increasing angle, the effect of the frictional

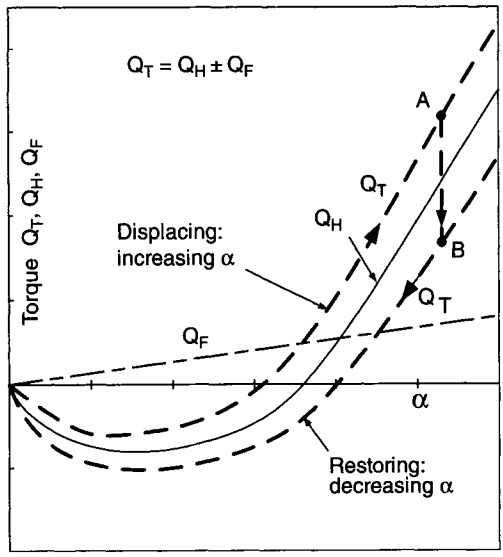

Figure 7.6 Effect of friction in bearings on rudder torque

torque Q_F is to decrease the initial negative torque and increase the positive torque at larger angles. When the rudder action is reversed, say at point A, the torque drops to point B on the restoring curve. When the rudder is restoring, with decreasing angle (rudder effectively driving the steering gear), the effect of Q_F is to decrease Q_T at positive torque and increase Q_T at negative torque. Note that, in reality, there will be a complete reversal of sign for the restoring Q_T at point B, which for schematic purposes, is not shown in Figure 7.6.

The frictional torque Q_F is derived from the reactions in the rudder stock bearings due to the total rudder normal force N. The frictional torque at each bearing is then the resultant force multiplied by the coefficient of friction multiplied by the bearing turning radius. For the case of the spade rudder, Figure 7.7:

$$Q_F = \mu_B R_1 N \left[\frac{y_1 + y_2}{y_3} \right] + \mu_B R_2 N \left[\frac{y_1 + y_2 + y_3}{y_3} \right] \tag{7.14}$$

where μ_B is the coefficient of friction of the bearing material and R_1 and R_2 are the radii of the bearings. Typical values of μ_B for sleeve bearings are 0.1 for metals and 0.2 for synthetic materials, Taplin [7.20] and Harrington [7.24].

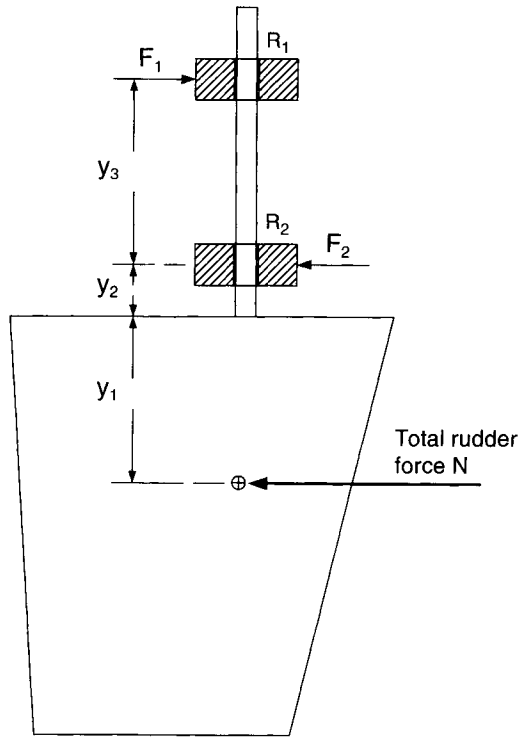

Figure 7.7 Resolution of forces at bearings

Harrington [7.24] uses a number of worked examples to illustrate the derived hydrodynamic and frictional torques for spade and semi-balanced skeg rudders. Taplin [7.20] includes calculations for frictional torque. The frictional torque Q_F is assumed linear with angle, Figure 7.6, and at 30–35° may be about 5–10% of the total torque Q_T. At 10–20°, when hydrodynamic torque Q_H can be very low or tending to zero (but the normal force is still present, Figure 7.4), Q_F will represent a much higher proportion of the total torque. The effect of friction in the rudder bearings is included in example application 2 in Chapter 11.

(D) *Rudder rate*: The steering gear torque may be further influenced by the rate of change of rudder angle. The time to change heading and abilities such as zig–zag overshoot characteristics are affected by rudder deflection rate, although the rate has no influence on the diameter of the steady turn. Minimum rudder rates of 2½°/s are required by regulatory bodies and classification societies. That is typically putting the rudder over from 35° one side to 35° the other side in 30 s, or 35° one side to 30° the other side in 28 s. Such rudder rates are generally acceptable for most ship types. Ideally, a fast rudder rate is called for initially, with rudder angle rising to just below stall. As drift angle develops, the rudder angle would be increased such that the effective angle remains just below stall. As pointed out by Mandel [7.15], this ideal goal is generally not possible.

Mandel [7.15] investigated the influence of changes in rudder rate, based on the time to change the heading by 30°, resulting in a trend shown schematically in Figure 7.8. It was found that increases in rudder rate provided greater improvements in shorter ships than larger ones. It was also deduced that, based on the results of the investigation, a good rudder rate to select for most ships would be a rate that corresponds to about 15° rudder deflection per ¼ ship length of travel, and indicates this would amount to a rudder rate of about 5°/s for a 122 m, 20 knot ship. This is in the area where the curve in Figure 7.8 flattens and further increases in rate are not very effective. Mandel concluded that most ships will have a rate somewhat lower than 5°/s. The effect of rudder rate was examined in some detail by Eda and

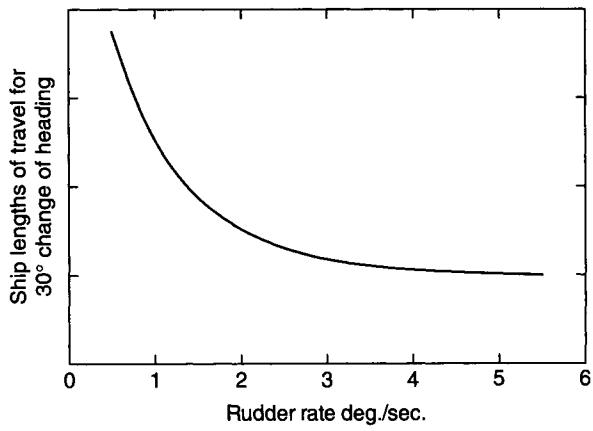

Figure 7.8 Influence of rudder rate

Crane [7.41] and Eda [7.42, 7.43]. Their results indicate that beyond about 3°/s, further improvements become very small. It should be finally noted that increased rudder rate will increase the torque to a certain extent and increase the load on the steering gear.

(E) *Full-scale tests*: In making predictions for full-scale rudder performance, note will be made of the relevant Reynold's number and whether any correction for scale effects should be included. Effects of Reynold's number are discussed in Section 5.3.2.

Many difficulties can arise when attempting to measure full-scale rudder forces and torques. Ideally, forces and torque would be measured using suitably sited strain gauges on the rudder and rudder stock, and such an approach was used in the trials reported by Becker and Brock [7.44]. Very few results of such detailed measurements have been published elsewhere. More normally, torque has to be measured indirectly using the pressures in the hydraulic rams of the steering gear. Further corrections then have to be made to allow for mechanical friction in the steering system and in the rudder stock bearings. The difficulties arising from this approach are discussed by Hagen [7.18], Taplin [7.45] and Harrington [7.24]. Son *et al.* [7.28] compare, for a large tanker, the sea-trial torque from the steering gear with a regression model of rudder torque.

In making a comparison of full-scale measurements with those predicted by model, care has to be taken with the measurement or prediction of the actual full-scale rudder angle of attack and inflow speed, allowing for wake, propeller slipstream, hull drift angle and change in rudder angle of attack as the ship turns. With careful consideration of all the corrections, reasonable correlation between model and full-scale can be achieved. The extended discussion to Harrington's paper covers most aspects of the problems associated with full-scale predictions and tests.

A further indirect approach to checking overall rudder forces is to compare the full-scale manoeuvring trial results, such as in reference [7.46], with those from a mathematical manoeuvring simulation that adequately models the rudder, such as in reference [7.47]. It has to be noted that, as this approach models the hull, propeller and rudder, interaction effects need to be modelled correctly, otherwise acceptable overall manoeuvring predictions may be obtained for the wrong reasons.

Full-scale tests on roll stabilisers can be more productive. The ship can be force rolled (in calm water) using the fins and the resulting roll angle compared with the design waveslope capacity of the fins (see Section 9.1.2).

7.3 Applications of numerical methods

Chapter 6 describes in some detail the application of numerical methods suitable for the design of control surfaces. Techniques reviewed include potential flow and Navier–Stokes methods, together with unsteady behaviour. Particular applications include the design of section shape, for example to delay stall or cavitation, together with the ability to determine surface pressures and load distributions for a wide range of shapes in the freestream and behind a propeller.

7.4 Guidelines for design

When considering the overall design process and in deciding the most appropriate rudder or control surface for a particular task, three complementary areas of knowledge can be used:

(1) Empirical knowledge derived from in-service experience but, more usually these days, from the results of model-scale experimentation of varying levels of complexity and expense. These are discussed in Chapter 5.
(2) Theoretical investigation, using dimensional analysis, that allows the categorisation of the appropriate flow regime and then adoption of a suitable mathematical approximation, as discussed in Chapter 6.
(3) The use of numerical methods to solve the many fluid dynamic equations required to discretise a complete domain, as discussed in Chapter 6.

The most effective design strategy will be one that permits an appropriate synthesis of the three areas in a suitable blend.

It is difficult to develop a universal guideline. As in the majority of designs, the quality and sophistication of the final product will depend on the resources made available, both in terms of expenditure associated with model testing (computational or experimental) and, most importantly, the amount of time available for work on the project.

References

7.1 Kinoshita, M. and Okada, S. On the twisting moment acting upon a ship's rudder stock. *International Shipbuilding Progress*, Vol. 2, No. 9, 1955, pp. 230–240.
7.2 Jöessel, Rapport sur des experiences relatives aux gouvernails. *Memorial du Genie Maritime*, Rapport 9, 1873.
7.3 Denny, M.E. The design of balanced rudders of the spade type. *Transactions of the Royal Institution of Naval Architects*, Vol. 63, 1921, pp. 117–130.
7.4 Baker, G.S. and Bottomley, G.H. Manoeuvring of ships. Part I – Unbalanced rudders of single screw ships. *Transactions of the Institute of Engineers and Shipbuilders in Scotland*, Vol. 65, 1921/22, pp. 522–583.
7.5 Bottomley, G.H. Manoeuvring of ships. Part II – Unbalanced rudders of twin screw ships. *Transactions of the Institute of Engineers and Shipbuilders in Scotland*, Vol. 67, 1923/24, pp. 509–559.
7.6 Bottomley, G.H. Manoeuvring of ships. Part III – Unbalanced rudders behind single screw ships, effect of varying fullness of form. *Transactions of the Institute of Engineers and Shipbuilders in Scotland*, Vol. 70, 1926/27, pp. 463–500.
7.7 Bottomley, G.H. Manoeuvring of ships. Part IV – Unbalanced rudders behind twin screw ships, effect of varying fullness of form. *Transactions of the Institute of Engineers and Shipbuilders in Scotland*, Vol. 74, 1930/31, pp. 94–123.
7.8 Bottomley, G.H. Manoeuvring of ships – Semi-balanced rudders of twin screw ships. *Transactions of the North East Coast Institution of Engineers and Shipbuilders*, Vol. 48, 1931/32, pp. 97–114.

7.9 Bottomley, G.H. Manoeuvring of single screw ships – The effect of rudder proportions on manoeuvring and propulsive efficiency. *Institution of Civil Engineers*, Selected Engineering Papers, No. 175, 1935, pp. 1–18.
7.10 Abell, T.B. Some model experiments on rudders placed behind a plane deadwood. *Transactions of the Royal Institution of Naval Architects*, Vol. 78, 1936, pp. 135–144.
7.11 Gawn, R.W.L. Steering experiments, Part I. *Transactions of the Royal Institution of Naval Architects*, Vol. 85, 1943, pp. 35–73.
7.12 Van Lammeren, W.P.A., Troost, L. and Koning, J.G. *Resistance, Propulsion and Steering of Ships*. The Technical Publishing Co. H. Stam-Haarlem, Holland, 1948.
7.13 Attwood, E.L. and Pengelly, H.S., revised by A.J. Sims. *Theoretical Naval Architecture*. Longmans, Green and Co. London, 1953.
7.14 Lamb, B.J. and Cook, S.B. A practical approach to rudder design. *Shipbuilding and Shipping Record*. September 1961, pp. 334–336.
7.15 Mandel, P. Some hydrodynamic aspects of appendage design. *Transactions of the Society of Naval Architects and Marine Engineers*, Vol. 61, 1953, pp. 464–515.
7.16 Jaeger, H.E. Approximate calculation of rudder torque and rudder pressures. *International Shipbuilding Progress*, Vol. 2, No. 10, 1955, pp. 243–257.
7.17 Gover, S.C. and Olsen, C.R. A method for predicting the torque of semi-balanced centreline rudders on multiple-screw ships. *DTMB Rep. 915*, 1954.
7.18 Hagen, G.R. A contribution to the hydrodynamic design of rudders. Ministry of Defence, *Third Ship Control Systems Symposium*, Bath, September 1972.
7.19 Whicker, L.F. and Fehlner, L.F. Free stream characteristics of a family of low aspect ratio control surfaces for application to ship design. *DTMB Report 933*, December 1958.
7.20 Taplin, A. Notes on rudder design practice. *DTMB Report 1461*, October 1960.
7.21 Romahn, K. and Thieme, H. On the selection of balance area for rudders working in the slipstream (in German). *Schiffstechnic*, No. 21, 1957.
7.22 Thieme, H. Design of ship rudders. *Jarbuch der Schiffbautechnischen Gesellschaft*, Vol. 56, 1962 or DTMB Translation No. 321, 1965.
7.23 Okada, S. On the performance of rudders and their designs. *The Society of Naval Architects of Japan*, 60th Anniversary Series, Vol. 11, 1966, pp. 61–137.
7.24 Harrington, R.L. Rudder torque prediction. *Transactions of the Society of Naval Architects and Marine Engineers*, Vol. 89, 1981, pp. 23–90.
7.25 Millward, A. The design of spade rudders for yachts. *Southampton University Yacht Research Report*, SUYR No. 28, 1969.
7.26 Molland, A.F. Rudder design data for small craft. University of Southampton, *Ship Science Report* No. 1/78, 1978.
7.27 Brix, J. (ed.) *Manoeuvring Technical Manual*, Seehafen Verlag, Hamburg 1993.
7.28 Son, D.I., Ahn, J.H. and Rhee, K.P. An empirical formula for steering gear torque of tankers with a horn rudder. Proceedings of *the 8th International Symposium on Practical Design of Ships and Mobile Units, PRADS'2001*, Shanghai, 2001.
7.29 Kresic, M. Estimating hydrodynamic force and torque acting on a horn-type rudder. *Marine Technology*, Vol. 39, No. 2, April 2002, pp. 118–136.

7.30 Molland, A.F. A method for determining the free-stream characteristics of ship skeg-rudders. *International Shipbuilding Progress*, Vol. 32, No. 370, June 1985 pp. 138–150.
7.31 Goodrich, G.J. and Molland, A.F. Wind tunnel investigation of semi-balanced ship skeg-rudders. *Transactions of the Royal Institution of Naval Architects*, Vol. 121, 1979, pp. 285–307.
732 Molland, A.F. and Turnock, S.R. Flow straightening effects on a ship rudder due to upstream propeller and hull. *International Shipbuilding Progress*, 49, No. 3, 2002, pp. 195–214.
7.33 Smithwick, J.E.T. *Enhanced design performance prediction method for rudders operating downstream of a propeller.* Ph.D. Thesis, University of Southampton, UK, 2000.
7.34 Molland, A.F., Turnock, S.R. and Smithwick, J.E.T. Design studies of the manoeuvring performance of rudder–propeller systems. Proceedings of *the 7th International Symposium on Practical Design of Ships and Mobile Units, PRADS '98*, The Hague, The Netherlands, September 1998, pp. 807–816.
7.35 Lloyds Register of Shipping. *Rules and Regulations for the Classification of Ships*, Ship Control Systems, Part 3, Chapter 13, July 2005.
7.36 DNV *Rules for Classification of Ships*, Part 3, Chapter 3, Hull Equipment and Safety, Det Norske Veritas, Oslo, January 2006.
7.37 American Bureau of Shipping. *Guide for building and classing Motor Pleasure Yachts.* 1990.
7.38 American Bureau of Shipping. *Guide for building and classing Offshore Racing Yachts.* 1994.
7.39 Germanischer Lloyd. *Rules for Classification and Construction, 2006.*
7.40 ISO *Draft International Standard: Hull Construction – Scantlings – Rudders.* ISO/DIS 12215–12218, 2005.
7.41 Eda, H. and Crane, C.L. Steering characteristics of ships in calm water and in waves. *Transactions of the Society of Naval Architects and Marine Engineers*, Vol. 73, 1965, pp. 135–177.
7.42 Eda, H. Notes on ship controllability. *Society of Naval Architects and Marine Engineers Bulletin* No. 1-41, April 1983.
7.43 Eda, H. Shiphandling simulation study during preliminary ship design. Proceedings of *Fifth CAORF Symposium*, Kings Point, New York, May 1983.
7.44 Becker, L.A. and Brock, J.S. The experimental determination of rudder forces during trials of USS Norfolk. *Transactions of the Society of Naval Architects and Marine Engineers*, Vol. 66, 1958, pp. 310–344.
7.45 Taplin, A. Sea trials for measuring rudder torque and force. Proceedings of *Fourth Ship Control Systems Symposium.* Royal Netherlands Naval College, The Hague. Vol. 5. 1975, pp. 99–115.
7.46 Clarke, D., Patterson, D.R. and Woooderson, R.K. Manoeuvring trials with the 193,000 Tonne deadweight tanker 'Esso Bernicia'. *Transactions of the Royal Institution of Naval Architects*, Vol. 114, 1973, pp. 89–109.
7.47 Molland, A.F., Turnock, S.R. and Wilson, P.A. Performance of an enhanced rudder force prediction model in a ship manoeuvring simulator. Proceedings of *International Conference on Marine Simulation and Ship Manoeuvrability, MARSIM '96*, Copenhagen, Denmark, 1996, pp. 425–434.